Combination Antisense Treatment for Destructive Exon Skipping of Myostatin and Open Reading Frame Rescue of Dystrophin in Neonatal *mdx* Mice

Ngoc B Lu-Nguyen[1], Susan A Jarmin[1], Amer F Saleh[2,3], Linda Popplewell[1], Michael J Gait[2] and George Dickson[1]

[1]*School of Biological Sciences, Royal Holloway, University of London, Surrey, UK;* [2]*Medical Research Council, Laboratory of Molecular Biology, Francis Crick Avenue, Cambridge Biomedical Campus, Cambridge, UK;* [3]*Current address: AstraZeneca R&D, Discovery Safety, Drug Safety and Metabolism, Alderley Park, Macclesfield, UK*

The fatal X-linked Duchenne muscular dystrophy (DMD), characterized by progressive muscle wasting and muscle weakness, is caused by mutations within the *DMD* gene. The use of antisense oligonucleotides (AOs) modulating pre-mRNA splicing to restore the disrupted dystrophin reading frame, subsequently generating a shortened but functional protein has emerged as a potential strategy in DMD treatment. AO therapy has recently been applied to induce out-of-frame exon skipping of myostatin pre-mRNA, knocking-down expression of myostatin protein, and such an approach is suggested to enhance muscle hypertrophy/hyperplasia and to reduce muscle necrosis. Within this study, we investigated dual exon skipping of dystrophin and myostatin pre-mRNAs using phosphorodiamidate morpholino oligomers conjugated with an arginine-rich peptide (B-PMOs). Intraperitoneal administration of B-PMOs was performed in neonatal *mdx* males on the day of birth, and at weeks 3 and 6. At week 9, we observed in treated mice (as compared to age-matched, saline-injected controls) normalization of muscle mass, a recovery in dystrophin expression, and a decrease in muscle necrosis, particularly in the diaphragm. Our data provide a proof of concept for antisense therapy combining dystrophin restoration and myostatin inhibition for the treatment of DMD.

Received 23 January 2015; accepted 28 April 2015; advance online publication 16 June 2015. doi:10.1038/mt.2015.88

INTRODUCTION

Duchenne muscular dystrophy (DMD) is a recessive X-linked muscle disease, affecting 1 in 3,500 live male births. Almost 30 years since the discovery of the *DMD* gene,[1] there has been no cure for this fatal disorder. Current treatments have shown alleviation in the dystrophinopathic symptoms but failed in halting the disease progression. Gene therapy-based studies, in particular an approach using antisense oligonucleotides (AOs), however, have recently held promise for DMD patients. This therapy uses small oligonucleotides to correct frame-shifting or nonsense mutations of the *DMD* gene by skipping a mutated exon or exons which disrupt the reading frame in such a way that it restores the reading frame of the dystrophin transcript, leading to synthesis of shortened but functional dystrophin protein. Encouraging results have been demonstrated in murine[2,3] and canine models[4] of DMD and have been translated into clinical trials[5–7] with minor safety concerns. However, clinical application so far has used either phosphorodiamidate morpholino oligomer (PMO) or 2′-O-methyl-phosphorothioate (2′-OMePS) AO (clinicaltrials.gov identifiers NCT01254019, NCT01396239) that usually requires high and frequently repeated dosages due to poor cell uptake and rapid renal clearance of the AOs.[5] Importantly, these AOs induced restoration of dystrophin expression in skeletal muscles but failed in cardiac tissue,[8] unless extremely high doses were used,[9] while cardiomyopathy is one of the two causes of death in DMD. Researchers therefore have developed a new generation of AOs, conjugated to cell penetrating peptides, *i.e.*, PMOs conjugated with an arginine-rich B peptide (BPMOs). Preclinical tests in DMD mouse models have demonstrated therapeutic effects of BPMOs were far more efficient than of unconjugated PMOs when used at the same dose,[10] and interestingly with dystrophin expression in body-wide skeletal plus cardiac muscles.[11]

Therapeutic benefits of antisense therapy-mediated dystrophin expression however depend on the severity of the disease at the time the treatment is initiated. Indeed, depletion in the muscle fiber number, reduction in the muscle mass together with compromised integrity in the fiber structure and formation of muscle fibrosis in late stages of DMD cannot be targeted only by recovering dystrophin levels.[12] Hence, knock-down of myostatin expression, a negative regulator of skeletal muscle growth and differentiation[13] and an enhancer of the proliferation of muscle fibroblasts,[14] has been suggested as a potential adjunct therapy for DMD. We have initially published that AO-induced out-of-frame skipping of myostatin stimulated hypertrophy in treated tibialis anterior muscles of wild-type mice.[15] We and others have further investigated dual skipping of dystrophin and myostatin in mouse and human dystrophic cells[16] and in a *mdx* mouse model of DMD,[10] confirming the efficacy of the combined antisense therapy with no interference between the two AOs. However, BPMO-induced exon skipping levels of myostatin in treated mice were four to five times lower

Correspondence: George Dickson, School of Biological Sciences, Royal Holloway, University of London, Egham, Surrey, TW20 0EX, UK. E-mail: G.Dickson@rhul.ac.uk

than that of dystrophin although both BPMOs were used at the same dose, resulting in no significant difference in the therapeutic effects between single and dual treatments. A tentative explanation for such failure can be that the treatment started 6 weeks after animal birth, rather than at birth, when negative effects of the disease began to accumulate,[17,18] reducing or interfering with the therapeutic benefit. A possible inadequate dose of BPMO-myostatin is an additional reason for the lack of success. To circumvent this, we investigated here the effects of a dual exon skipping approach in neonatal *mdx* through regular systemic administration of the BPMOs. As expected, the intervention at very early stage of the disease enhanced the therapeutic benefit. This study importantly establishes that AO-mediated downregulation of myostatin expression can be a synergistic therapy with AO-induced restoration of dystrophin level for the treatment of DMD.

RESULTS

RT-PCR demonstrating skipping of dystrophin and myostatin pre-mRNAs

In order to confirm our previous findings[10] and to further enhance the therapeutic benefits of AO-induced dual exon skipping of dystrophin and myostatin pre-mRNAs, we investigated here a

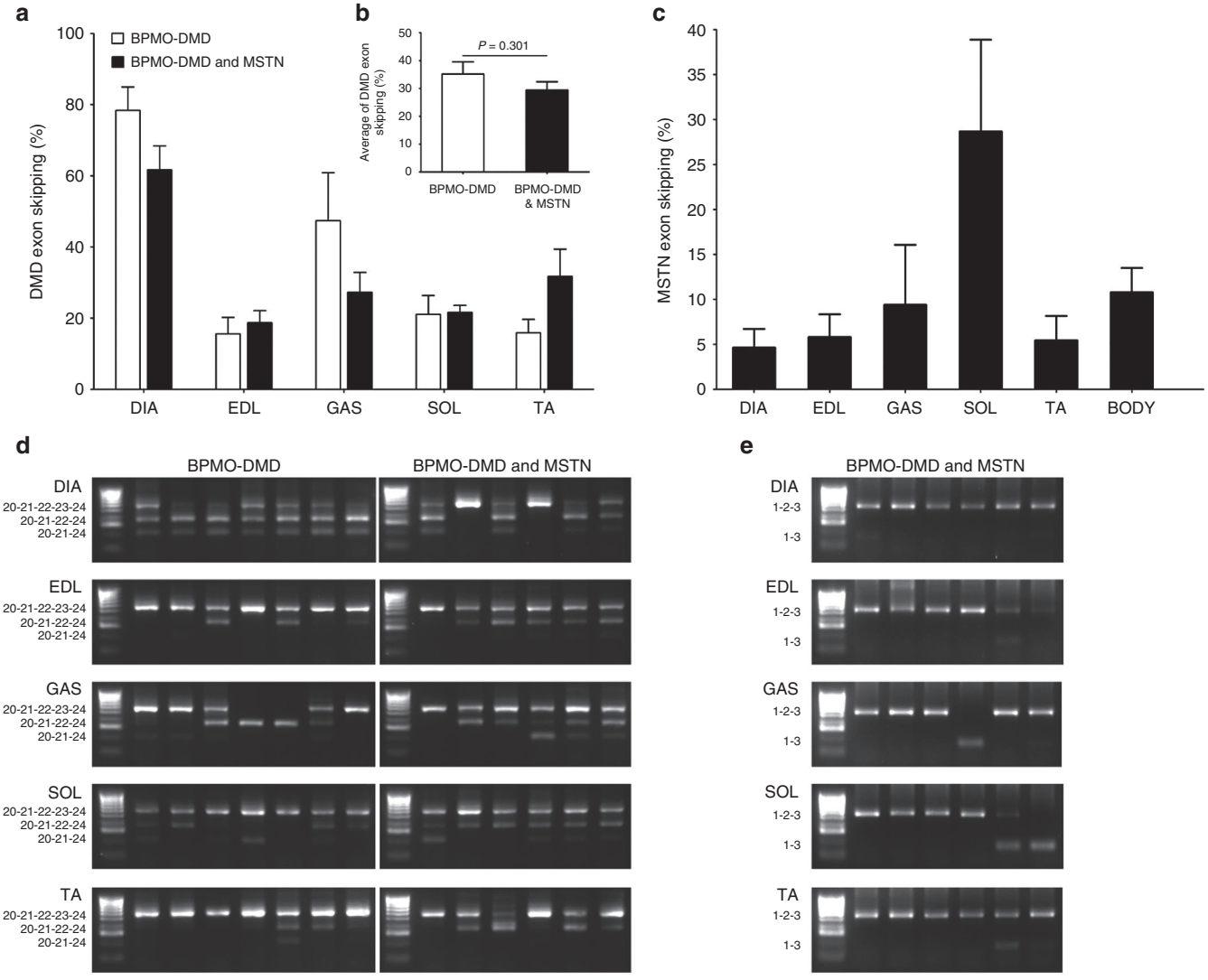

Figure 1 Confirming BPMO-induced dystrophin and myostatin exon skipping through RT-PCRs. Neonatal *mdx* were injected with BPMO-DMD (10 mg/kg, $n = 7$) or a cocktail of BPMO-DMD and BPMO-MSTN (10 mg/kg each BPMO, $n = 6$). Intraperitoneal injection was performed on day 0 and was repeated every 3 weeks afterwards. Mice were sacrificed at week 9. Total RNA from the diaphragm (DIA), extensor digitorum longus (EDL), gastrocnemius (GAS), soleus (SOL), and tibialis anterior (TA) was excised and RNA extracted for semi-nested dystrophin RT-PCRs or nested myostatin RT-PCRs. (**a**) Levels of dystrophin exon skipping within individual muscles and (**b**) an average of dystrophin exon skipping from five muscles are displayed. (**c**) Efficiency of myostatin exon skipping from five examined muscles and as an average of those values (body). The efficiency of dystrophin or myostatin exon skipping was evaluated through densitometric analysis of RT-PCR products as a percentage of the density of skipped products against the density of both skipped and unskipped products. Results shown in (**a–c**) were from two separate RT-PCRs. Data are expressed as means ± standard error of the mean (SEM); error bars represent the SEM. Statistical analysis in **a, b** was performed by two-tailed Student's *t*-test with no significant difference was detected. (**d,e**) Representative RT-PCR products demonstrate dystrophin and myostatin exon skipping, respectively. PCR products were loaded onto 2% agarose gel; each lane displays the result from individual mouse; HyperLadder IV was used as a molecular size standard. Exons included in PCR product bands shown to the left of each gel.

combined therapy in p0 *mdx* mice through regular intraperitoneal (i.p.) injection. *Mdx* neonates were injected with 10 mg/kg of BPMO-DMD (n = 7) or a mixture of BPMO-DMD and BPMO-MSTN, 10 mg/kg each BPMO (n = 6). After three injections on day 0, weeks 3 and 6, the diaphragm (DIA) and four skeletal muscles, including the extensor digitorum longus (EDL), gastrocnemius (GAS), soleus (SOL), and tibialis anterior (TA), were collected. RNA extraction and subsequent reverse transcription polymerase chain reactions (RT-PCRs) were performed. Representative PCR products (**Figure 1d**) indicated efficient skipping of DMD exon 23 (or both exons 22 and 23) in all examined tissue. A further analysis clarified the skipping levels of dystrophin pre-mRNA were in a range of 16–78%, with the highest value in the diaphragm (78.4 ± 6.6%), (**Figure 1a**). We observed no statistical difference in the skipping efficiency between BPMO-DMD administered alone and in combination with BPMO-MSTN, at individual muscle level (**Figure 1a**) or at systemic level (**Figure 1b**), suggesting no interference between the two oligomers in the dual therapy. Skipping levels of myostatin, however, was threefold less than those of dystrophin. The highest skipping at 28.7 ± 10.2% was detected in the soleus whereas surprisingly the diaphragm displayed the lowest skipping at 4.6 ± 2.1% (**Figures 1c**,**e**). Our results demonstrated initial effects of the antisense treatment although with a variability in the skipping levels possibly due to systemic i.p. administration of the BPMOs.

Substantial expression of dystrophin in the diaphragm of BPMO-injected *mdx*

As described in the previous section, DIA, GAS, and TA muscles were harvested from treated *mdx* mice. The amount of dystrophin within these muscles was then evaluated by western blotting, with detectable expression observed in only the diaphragm (**Figure 2a**). Subsequent quantification of dystrophin expression, in comparison with C57 control samples (considered as 100%), confirmed 15.7 ± 6.2% and 43.7 ± 19.4% dystrophin presented in BPMO-DMD- and BPMO-DMD and -MSTN-treated muscles, respectively (**Figure 2b**). Although the level of dystrophin from *mdx* receiving the combined treatment appeared three times higher than that from BPMO-DMD-injected group, statistical analysis confirmed no significant difference between the two treatment sets (P = 0.17, two-tailed Student's t-test).

In addition to western blot quantification, dystrophin expression was ascertained by immunohistochemistry staining (**Figure 3**). As expected, the intensity of dystrophin within C57 samples was obvious whereas nearly no dystrophin-positive fibers were detected from saline-injected *mdx* muscles. In BPMO-receiving groups, the levels of dystrophin intensity were variable among the five tissues assessed. However, dystrophin expression within diaphragm sections was the highest and comparable to C57 control samples. Hence, histological analysis provided consistent results with western blot quantification, suggesting that AO therapy in neonatal *mdx* effectively rescues dystrophin synthesis, predominantly in the diaphragm, maybe due to the administration route of the BPMOs.

Antisense-mediated treatment ameliorated the pathology of DMD, significantly in the diaphragm

Following encouraging results at transcriptional and translational levels, we investigated the therapeutic benefit of antisense therapy on the diaphragm at the cellular level. Laminin staining

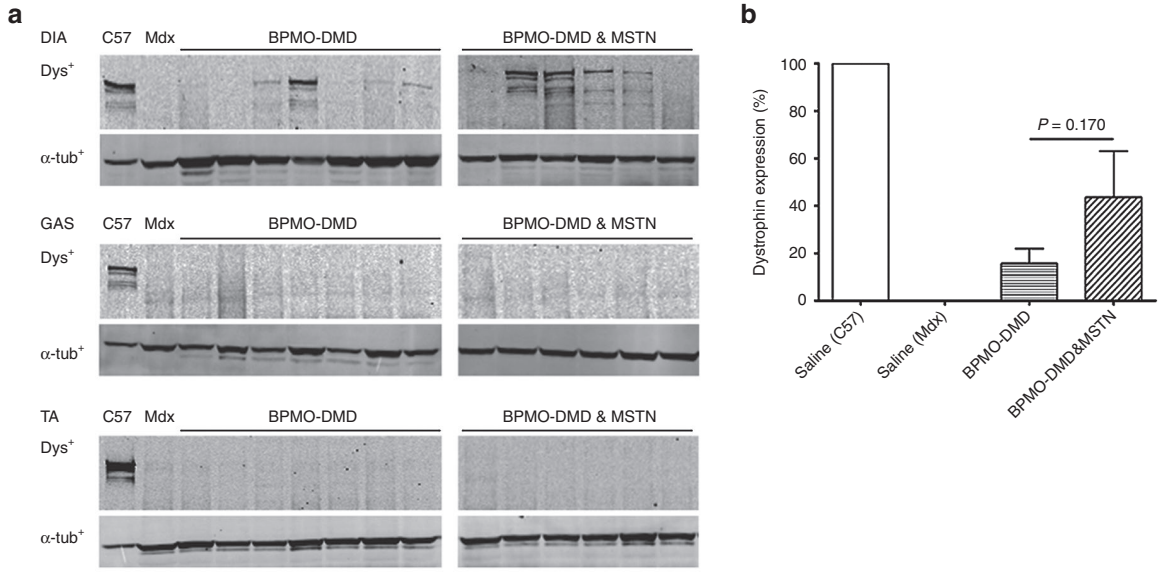

Figure 2 Western blotting demonstrates a recovery in dystrophin expression of treated *mdx* mice. Following i.p. administration (at day 0, weeks 3 and 6) of BPMO-DMD (10 mg/kg, n = 7) or a cocktail of BPMO-DMD and BPMO-MSTN (10 mg/kg each BPMO, n = 6), the diaphragm (DIA), gastrocnemius (GAS), and tibialis anterior (TA) were excised at week 9. Proteins from these muscles were then extracted. (**a**) Expression of dystrophin (dys$^+$) was confirmed by western blot analysis. Each lane represents a sample from an individual mouse. Proteins from muscle type-matched of saline-injected C57 and *mdx* were loaded as positive and negative controls, respectively. α-tubulin (α-tub$^+$) was used as an internal loading control for western blot. (**b**) An evaluation of dystrophin levels expressed in the diaphragm. Following a densitometric analysis, the intensity of dys$^+$ patterns was normalized to the intensity of corresponding α-tub$^+$ patterns; the results were expressed as a percentage of the value from C57 sample obtained in the same way (which was considered as 100%). Data are shown as means ± standard error of the mean (SEM), with error bars representing the SEM. Statistical comparison was analyzed by two-tailed Student's t-test.

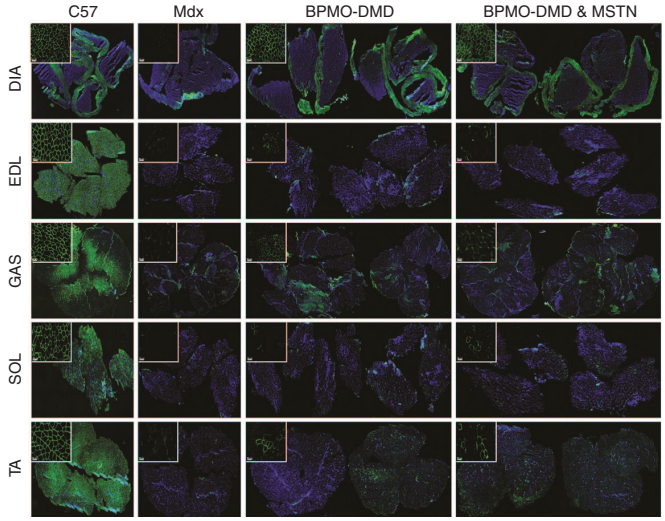

Figure 3 Dystrophin expression within skeletal muscle sections is ascertained by immunohistochemistry staining. *Mdx* neonates were injected (i.p.) with BPMO-DMD (10 mg/kg, $n = 7$), a cocktail of BPMO-DMD and BPMO-MSTN (10 mg/kg each BPMO, $n = 6$), or volume-matched sterile saline ($n = 4$); a group of C57 ($n = 5$) receiving i.p. injection of saline was used as a positive control. The injection was performed every 3 weeks. Muscles were collected at week 9 and were subsequently sliced at 10 µm thickness. Representative mosaic images demonstrating dystrophin expression from BPMO-injected *mdx* or C57 muscles are shown as in groups of treatment. Cell images at higher magnification are shown in top-left insets at scale bar = 50 µm. Dystrophin-positive fibers were stained in green. Nuclei were stained in blue with DAPI (4,6-diamidino-2-phenylindole). DIA, diaphragm; EDL, extensor digitorum longus; GAS, gastrocnemius; SOL, soleus; TA, tibialis anterior.

was used to reveal the perimeter, especially of dystrophic fibers (**Figure 4a**). According to a measurement of the minimal Feret's diameter of the fibers, a shift was observed in the distribution of BPMO-treated diaphragm fibers, reverting towards the wild-type of C57 fibers (**Figure 4b**). A subsequent evaluation demonstrated a significant reduction of 15 and 30% in the variance coefficient of the Feret's diameter of BPMO-DMD and BPMO-DMD and -MSTN groups, respectively, as compared to saline-injected *mdx* (**Figure 4c**). Nonetheless, such changes did not normalize to wild-type C57 controls. Since DMD is characterized as a muscle wasting disorder, the number of fibers within each diaphragm section was additionally quantified. In comparison to C57 samples, we observed a significant decrease only in the fiber number of nontreated *mdx* ($P = 0.01$, two-tailed Student's *t*-test), (**Figure 4d**). As further assessment of the effects on dystrophic muscles previously undergoing muscle degeneration and regeneration, we calculated the prevalence of fibers having centralized nuclei (as percentage of the total number of fibers) within each section (**Figure 4e**). Healthy C57 muscle displayed less than 1% centronucleated fibers while as expected the percentage in untreated *mdx* muscle was 43.4 ± 1.7%. This reduced to 27.2 ± 3.2 and 13.8 ± 3.0% after treatment with BPMO-DMD or BPMO-DMD and -MSTN, respectively. Moreover, a statistical difference ($P = 0.004$, two-tailed Student's *t*-test) between the two BPMO-treated groups was identified, with reduced centronucleation in the BPMO-DMD and -MSTN group.

When this analysis was applied to the soleus muscle (where exon skipping of myostatin was most efficient among the five tissues assessed, which is possibly dependent on the fiber type) (**Figures 4f–j**), surprisingly, the frequency distribution of the minimal Feret's diameter (**Figure 4g**) and the variance coefficient values (**Figure 4h**) in *mdx* groups (both treated and nontreated) were as comparable as those from C57. On the contrary, a significant drop in the total fiber number (**Figure 4i**) and **a** resulting high proportion of fibers having centralized nuclei (**Figure 4j**) was seen in *mdx* muscles when compared to healthy controls. Among the *mdx* groups, the fiber values from BPMO-DMD group were not significantly different in comparison with those from BPMO-DMD and -MSTN- or nontreated group, whereas administration of BPMO-DMD and -MSTN provided an obvious reduction in the percentage of centrally nucleated fibers, as compared to nontreated *mdx*. Hence, the data from histological analysis confirmed the therapeutic effects of these antisense therapies. AO-induced exon skipping restoration of the reading frame of dystrophin pre-mRNA ameliorated the pathology of DMD. The benefit, moreover, was significantly enhanced when combined with destructive exon-skipping inhibition of myostatin.

Effects of antisense therapy on body and muscle mass

Neonatal *mdx* males received either 10 mg/kg of BPMO-DMD ($n = 7$) or a combination of 10 mg/kg BPMO-DMD and 10 mg/kg BPMO-MSTN ($n = 6$) on day 0, week 3 and week 6. The body weight was recorded every 2 weeks and was normalized to the birth weight (**Figures 5a,b**). Four weeks following the first injection, we observed some changes in treated *mdx* mice compared with saline-injected age-matched *mdx* ($n = 4$) or C57 ($n = 5$) subjects. However, from week 6 onwards, *mdx* mice (regardless of the treatment) displayed similar weight gain.

All mice were sacrificed at week 9. The mass of five muscle types, including DIA, EDL, GAS, SOL, and TA were evaluated (**Figure 5c**). In all tissues examined, muscle mass from *mdx* mice, both treated and nontreated, was heavier than that from wild-type animals. Nevertheless, after being normalized to the final body weight, the differences were observed in only large muscles, *i.e.*, DIA, GAS, and TA (**Figure 5d**). Significant changes between BPMO-treated *mdx* and nontreated *mdx* or C57 were seen, although limited, in the DIA (**Figures 5c,d**). A further analysis of the locomotor behavior of BPMO-injected animals demonstrated significantly normalized dystrophic phenotype of the *mdx* mice relative to the C57 controls, *i.e.*, total mobile counts, static time (**Supplementary Table S1**). These results ascertain the effects of AO therapy and provide a support for the treatment combining rescue of dystrophin and knockdown of myostatin.

DISCUSSION

Following our previous encouraging findings,[10,15] we investigated the effect of antisense-mediated dual exon skipping of dystrophin and myostatin pre-mRNAs in neonatal *mdx* mice. After three triweekly injections, we detected exon skipping of dystrophin (16–78%) and myostatin (5–29%) in all examined BPMO-treated muscles despite a high variability in the skipping level between muscle types and between subjects receiving the same treatment. A corresponding enhanced dystrophin

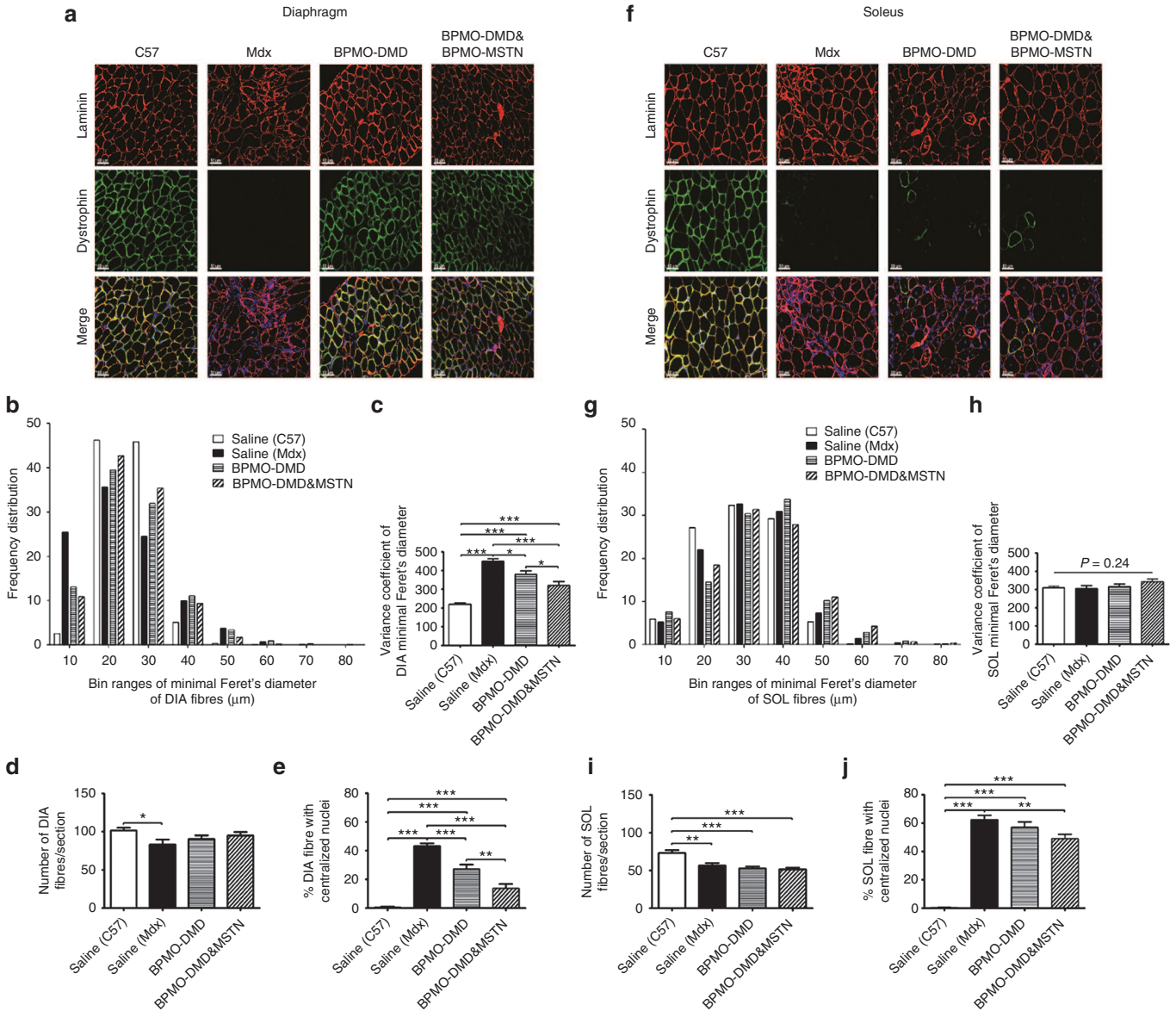

Figure 4 Effects of antisense therapy on diaphragm and soleus muscles. Either BPMO-DMD ($n = 7$) or a cocktail of BPMO-DMD and BPMO-MSTN ($n = 6$) was administered into *mdx* neonates at day 0, weeks 3 and 6. Following the same procedure, volume-matched saline was injected into another *mdx* group for negative control ($n = 4$) and into a C57 group for positive control ($n = 5$). At week 9 of age, muscles were harvested and sectioned at 10 µm thickness. Representative cell images from (**a**) diaphragm and (**f**) soleus sections are shown respectively. Laminin-positive fibers were stained in red while dystrophin-positive fibers were stained in green. Nuclei were stained in blue with DAPI. Scale bar = 50 µm. (**b,g**) Results from analysis of frequency distribution of the minimal Feret's diameter and (**c,h**) the variance coefficient of the Feret's diameter are displayed in turn for diaphragm and soleus fibers, as arbitrary units. (**d,i**) The total number of fibers and (**e,j**) the prevalence of centronucleated fibers (as percentage of the total fiber number) within each section of (**d,e**) the diaphragm or (**i,j**) the soleus are shown. Data are expressed as means ± standard error of the mean (SEM), with error bars representing the SEM. Significant differences were assessed by one-way analysis of variance followed by Bonferroni's *post-hoc* test; significant levels were set at $^{*}P < 0.05$, $^{**}P < 0.01$, $^{***}P < 0.001$.

expression of 16–44% (compared with wild-type control) was quantified by western blotting, and was ascertained by immunohistochemistry analysis. This led to muscle normalization toward the wild-type properties indicated by reduced disorganized fiber structure and fiber centronucleation. Such promising results were predominantly seen in the diaphragm, with better effect seen in the group receiving both BPMO-DMD and -MSTN. Our data provide a strong support for antisense therapy combining dystrophin restoration and myostatin inhibition for the treatment of DMD.

Among gene therapy-based approaches, which are potential treatments for DMD, antisense-induced exon skipping restoring the reading frame of dystrophin and the consequent dystrophin protein level has been the most promising strategy so far. This approach is indeed the only gene therapy to have entered phase 3 clinical trials for DMD. To date, however, there has been no study showing a complete rescue of dystrophin expression. Although a recovery over 20% of the normal dystrophin level (as we presented here) has been demonstrated to be sufficient to alleviate the dystrophic pathology, the lack of effect on muscle strength

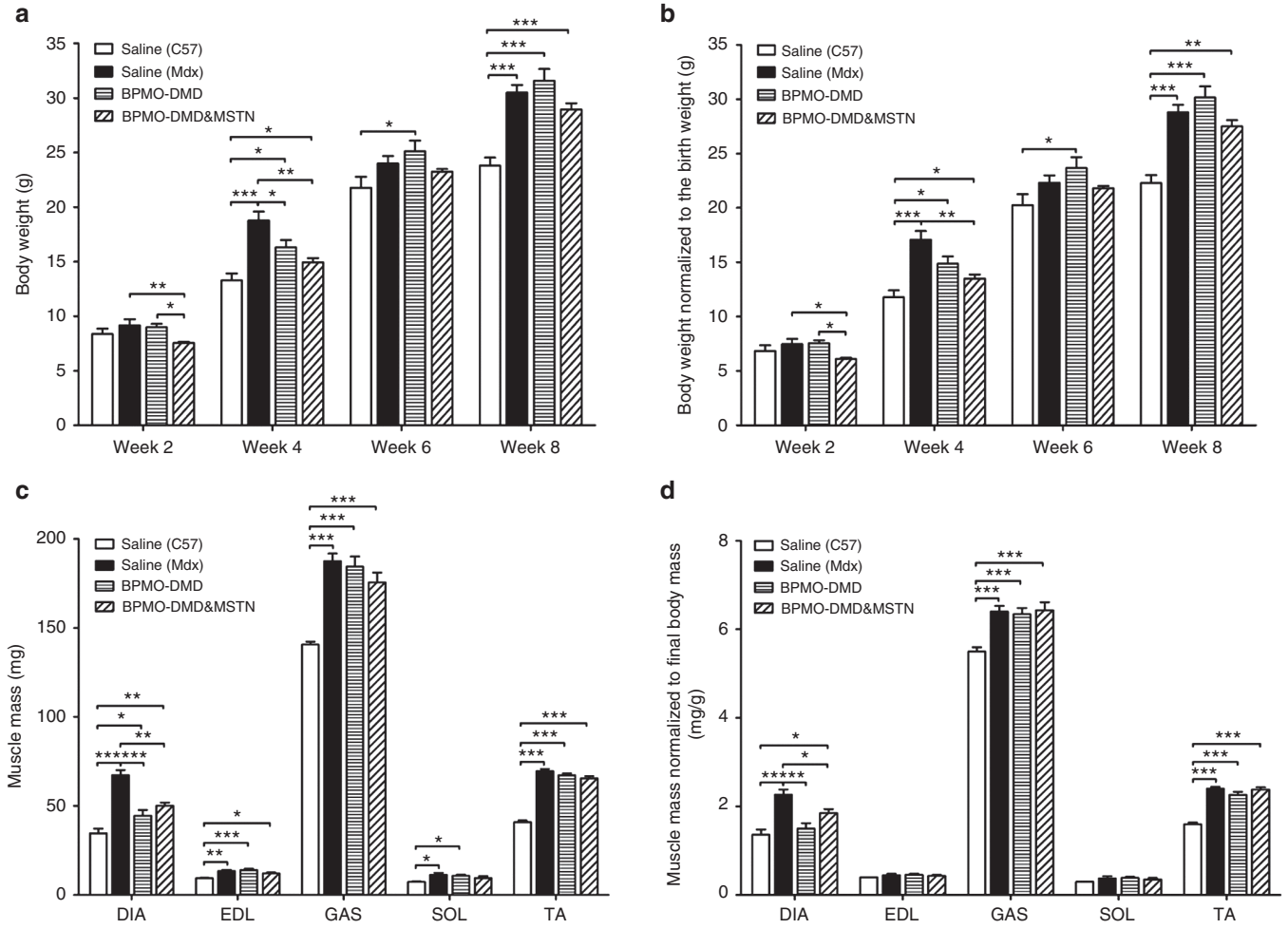

Figure 5 Effects of antisense oligonucleotide (AO) treatment on body and muscle mass. Neonatal mice received three i.p. injections on day 0, week 3, and week 6. *Mdx* were injected with either BPMO-DMD (10 mg/kg, $n = 7$) or a cocktail of BPMO-DMD and BPMO-MSTN (10 mg/kg each BPMO, $n = 6$); another group of *mdx* ($n = 4$) and a group of C57 ($n = 5$) neonates injected with volume-matched sterile saline acted as negative and positive controls, respectively. (**a**) Body weight assessed every 2 weeks is shown. (**b**) The weight at each 2-week time was then normalized to the birth weight. (**c**) Animals were sacrificed 3 weeks after the last injection; muscle mass of the diaphragm (DIA), extensor digitorum longus (EDL), gastrocnemius (GAS), soleus (SOL), and tibialis anterior (TA) is displayed. (**d**) Muscle mass was normalized to corresponding final body mass. Data are expressed as means ± standard error of the mean (SEM), with error bars representing the SEM. Statistical analysis was performed by one-way analysis of variance followed by Bonferroni's *post-hoc* test. Significant levels were set at $^*P < 0.05$, $^{**}P < 0.01$, $^{***}P < 0.001$.

has remained a challenge[19] which possibly depends on the stage (severity) of the disease when the treatment is applied.[12] Moreover, since the restored dystrophin protein is a truncated isoform with possibly a partial functionality, the therapy can only slow down not halt the disease progression. Hence, there is a growing consensus that the treatment for DMD needs to address the faulty *DMD* gene together with other aspects of the disease, *i.e.*, muscle fibrosis, muscle weakness.

In this study, combining restoration of dystrophin level with knocking-down myostatin expression enhanced the therapeutic benefit as compared with recovering dystrophin expression alone. The effect was predominant in the diaphragm, which could be beneficial in ameliorating the respiratory aspect of DMD, and is possibly due to the route of the administration used. However, the detection of only 5% myostatin exon skipping is not a strong evidence to support the positive effects of the combined treatment over the approach restoring dystrophin expression alone. We had reported[10] that after a single intramuscular injection of AOs, exon skipping of myostatin was detected immediately but weakened from week 4 whereas at that time the muscle mass began to increase significantly. Hence, the low level of myostatin skipping here might be a residue of a sufficient level that has already been beneficial for the dystrophic muscle. Possible underestimation of the skipping efficiency of myostatin is also hypothesized. Unlike in-frame skipping of dystrophin restoring the reading frame, out-of-frame skipped myostatin mRNA is nonsense and may be degraded immediately by intracellular nucleases. Thereby, measuring the remaining skipped product might be an inaccurate assessment. Future analysis may consider a more reliable quantification, *i.e.*, quantitative RT-PCR measuring the amount of full-length myostatin mRNA followed by a subsequent comparison between treated and nontreated samples.

Dumonceaux *et al.*[20] have demonstrated that myostatin blockage led to muscle hyperplasia; or muscle hypertrophy when it was in combination with rescue of dystrophin expression. A substantial increase in muscle mass, muscle fiber diameter and contractile

properties through downregulation of myostatin has been also reported in other preclinical and clinical trials.[10,21–23] In contrast, we observed the body weight, muscle mass, and muscle structure of treated mice normalized toward the wild-type properties. Indeed, an analysis at muscle level has indicated that knockdown of myostatin inhibited muscle degeneration and possibly thereby reduced muscle regeneration while no increase in muscle fiber size was detected. In regard to the body weight, within the first 4–6 weeks of development *mdx* mice are believed to be as heavy as wild-type animals.[18] However, the *mdx* in our study were already significantly heavier than the controls at week 4; only those receiving BPMOs displayed a comparable weight with control mice. This result indicated that therapeutic benefit could be achieved as early as after two injections, and in particular when the treatment was applied at early stage of the disease. However, we observed no difference in body weight between treated and untreated *mdx* from week 6 onwards. This may be because at that time the muscle necrosis has reached its peak[18] together with an effective innate muscle regeneration starting from weeks 3–4 (ref. 24) diminishing the therapeutic effect.

It is yet unclear what level of contribution myostatin knockdown makes to differences seen in this study which contradict the effects reported in other studies. Further investigation into downregulation of myostatin in *mdx* mice needs to be carried out to clarify this and to improve its effect on body-wide muscles. Importantly, since the gene sequence and the protein function of myostatin are highly conserved across species,[25–28] promising findings reported here can be feasibly translated into clinical trials in conjunction with the current dystrophin therapy to improve the treatment for DMD.

In summary, this study demonstrates that antisense therapy ameliorates the pathology of DMD, significantly in the diaphragm, which is beneficial for combating the respiratory aspect of the disease. The effect of dual treatment combining recovery of dystrophin expression and inhibition of myostatin expression is more effective than that of rescuing dystrophin levels alone. We also show that an intervention in early stages of DMD (*i.e.*, at birth) enhances the therapeutic benefits. Our data together strongly support clinical application of dual antisense therapy in DMD treatment.

MATERIALS AND METHODS

Antisense oligonucleotide preparation. PMO-MSTN (5′-AGCCCATCTT CTCCTGGTCCTGGGAAGG-3′) and PMO-DMD (5′-GGCCAAACCTC GGCTTACCTGAAAT-3′) that have been previously demonstrated to be biologically active in inducing skipping of myostatin exon 2 and dystrophin exon 23, respectively,[10] were purchased from GeneTools (Philomath, OR). The PMOs were then conjugated to an arginine-rich cell-penetrating peptide (B-peptide: RXRRBRRXRRBRXB) at the 3′-end of the PMO as previously described.[29] BPMOs were dissolved in sterile ddH_2O and were diluted in sterile 0.9% saline (Sigma, Dorset, UK) at a desired concentration immediately prior to an injection.

Animals and experimental design. Animal work was performed in accordance with the UK Animals (Scientific Procedures) Act, 1986. *Mdx* (C57BL/10ScSn-Dmdmdx) and C57BL/10 mice were bred inhouse and were maintained in a standard 12-hour light/dark cycle with free access to food and water. Mice were weaned at weeks 4–5 postnatal and were housed three to six individuals per cage. Since only males were used, mice within each experimental group were obtained randomly from two litters. The experiment included three *mdx* groups receiving either 10 mg/kg BPMO-DMD (n = 7), a combination of 10 mg/kg BPMO-DMD and 10 mg/kg BPMO-MSTN (n = 6), or volume-matched sterile saline (Sigma), (n = 4); and one C57 group injected with volume-matched sterile saline (n = 5) acted as a control. Intraperitoneal injections were administered at day 0, week 3, and week 6 of animal age. All mice were sacrificed at week 9.

Muscle tissue collection. Mice were sacrificed by exposure to a rising concentration of CO_2. From each mouse, the diaphragm—DIA, the extensor digitorum longus—EDL, the gastrocnemius—GAS, the soleus—SOL, and the tibialis anterior—TA were collected. Tissue from one side of the body was frozen immediately in liquid nitrogen for RNA and protein extraction while tissue from the other side was embedded in optimal cutting temperature medium (VWR, Leicestershire, UK) and subsequently frozen in liquid nitrogen-cooled isopentane (Sigma) for sectioning. All samples were kept at -80°C until use.

RNA extraction and RT-PCR analyzing exon skipping efficiency. RNeasy Fibrous Tissue kits (QIAgen, Manchester, UK) were used in RNA extraction. Muscle tissue was homogenized in the lysis buffer provided with the kit at 20 Hz for 2 minutes, twice, using a TissueLyser II (QIAgen). The total RNA was then extracted following the manufacturer's instructions. RNA quantification was performed on a ND-1000 NanoDrop spectrophotometer (Thermo Scientific, Leicestershire, UK). Five-hundred nanograms of extracted RNA were reverse transcribed by GeneScript RT-PCR kit (GeneSys, Surrey, UK) and resulting cDNA samples were then amplified through RT-PCRs. Two microlitres of RT-PCR products were used as templates in subsequent semi-nested (dystrophin exon skipping) or nested (myostatin exon skipping) PCRs. The final PCR products were then loaded onto 2% agarose gels. HyperLadder IV (Bioline, London, UK) was used as a size standard. Densitometric analysis of gel electrophoresis results was performed using GeneTools Image Analysis software 4.02 (Syngene, Cambridge, UK). The efficiency of dystrophin or myostatin exon skipping was evaluated as a percentage of the density of skipped products against the total density of unskipped and skipped products. RT-PCRs were performed in duplicate. Details of PCR programs and sequence of primers (MWG, Ebersberg, Germany) are available on request.

Protein extraction and western blotting quantifying dystrophin expression. Muscle tissue was homogenized in lysis buffer (0.15M NaCl, 0.05M HEPES (4-(2-Hydroxyethyl)piperazine-1-ethanesulfonic acid), 1% NP-40, 0.5% sodium deoxycholate, 0.1% SDS (sodium dodecyl sulfate), 0.01M EDTA (ethylenediaminetetraacetic acid)) containing protease inhibitors (Roche, Hertfordshire, UK) at 25 Hz for 2 minutes, twice, on a TissueLyser II (QIAgen). The supernatant, after centrifugation at 13,000 rpm/5 minutes/4 °C, was transferred to fresh prechilled 1.5 ml tubes. Quantifying the total protein was performed by *DC* Protein Assay (Bio-Rad, Hertfordshire, UK) following the manufacturer's instructions. Thirty micrograms total protein from C57 samples or 150 µg total protein from *mdx* samples were resolved on 3–8% Tris Acetate NuPage gels (Life Technologies, Paisley, UK). HiMark Pre-stained Protein Ladder (Life Technologies) was used as a size standard. The gels were run at 150 V for 1.5 hours then transferred to HyBond nitrocellulose membranes (GE Healthcare, Little Chalfont, UK) at 30 V for 2 hours. Protein transfer efficiency was immediately checked with Ponceau S staining. Membranes were then blocked in blocking buffer (1× phosphate-buffered saline (PBS), 0.05% Tween 20, 5% skimmed milk) for 1 hour, at room temperature. An overnight incubation at 4 °C with either monoclonal mouse anti-dystrophin 6C5 (1:100, Novocastra Laboratories, Newcastle upon Tyne, UK) or rabbit anti-α-tubulin (1:2,500, Abcam, Cambridge, UK) antibody was carried out. After three washes in 1× PBS/0.05% Tween 20 (1× PBS-T), the membranes were incubated with corresponding secondary antibody (1:10,000, LI-COR Biosciences, Cambridge, UK), either goat anti-mouse IRDye800 or goat anti-rabbit IRDye680. Western blot results were visualized on an Odyssey Infrared Imaging System (LI-COR Biosciences, Cambridge, UK). Densitometric analysis of dystrophin- and

α-tubulin-positive patterns was evaluated using ImageJ software (NIH, Bethesda, MD). The value of dystrophin intensity was then normalized to the value of corresponding α-tubulin intensity and was displayed as a percentage of the value of C57 samples obtained in the same way (considered as 100%). Reagents were purchased from Sigma, unless stated otherwise.

Muscle sectioning and immunohistochemical analysis. Tissue was cryo-sectioned on an OTF 5000 cryostat (Bright, Huntingdon, UK) at 10-µm thickness through the muscle length. Transverse sections were then fixed in ice-cold acetone and blocked in PBS containing 1% BSA, 1% goat serum, and 0.1% Triton X-100. Sections were subsequently incubated with rat anti-laminin antibody (1:1,000, Sigma) at 4 °C, overnight. Three washes in 1× PBS-T were completed prior to an incubation with goat anti-rat Alexa568 (1:1,000, Life Biotechnologies, Paisley, UK) in 1× PBS-T/1% goat serum for 1 hour. Subsequent dystrophin staining using Mouse-on-Mouse Fluorescein kit (Vector Laboratory, Peterborough, UK) was carried out following the manufacturer's instructions. Primary antibody was monoclonal mouse anti-dystrophin 6C5 (1:50, Novocastra Laboratories, Newcastle upon Tyne, UK) and secondary antibody was goat anti-mouse Alexa488 (1:1,000, Life Biotechnologies). An additional 15-minute staining with 1 µg/ml DAPI (4′,6-diamidino-2-phenylindole, Sigma) in 1× PBS-T/1% goat serum was performed. Sections were then mounted in Mowiol 4–88 medium (Sigma).

Cell image capture. Muscle sections were visualized under an inverted fluorescence Axio Observer D1 microscope. Single images were captured by an AxioCam MR3. These images were then used for fiber analysis or were automatically overlapped and stitched by AxioVision software to generate a mosaic image of each section. Equipment and software were purchased from Carl Zeiss (Cambridge, UK).

Histological analysis. Laminin staining (see previous section for materials and method) was used to identify the fiber perimeter. Incomplete fibers touching the edge of the image field were excluded. Semiautomatic quantification of the minimal Ferret's diameter of fibers was performed by ImageJ software (NIH). The variance coefficient of minimal Ferret's diameter from each section was then calculated as the ratio between the standard deviation (×1,000) and the mean of the diameter, and was expressed as arbitrary units. The number of fibers having internal nuclei within each section was counted manually and expressed as percentage of the total fiber number within that section.

Statistical analysis. Data were analyzed by GraphPad Prism5 software (San Diego, CA) and shown as the means ± standard error of the mean; error bars represent the standard error of the mean; "*n*" refers to the number of mice per group. Comparisons of statistical significance were assessed by one-way analysis of variance followed by Bonferroni's *post-hoc* test or by two-tailed Student's *t*-test. Significant levels were set at $^{*}P < 0.05$, $^{**}P < 0.01$, $^{***}P < 0.001$.

SUPPLEMENTARY MATERIAL

Table S1. Changes in mouse locomotor behavior after 8 weeks of treatment with BPMOs.

ACKNOWLEDGMENTS

The authors thank the Muscular Dystrophy UK for financial support. Work in the Gait laboratory is supported by the Medical Research Council (Unit program U105178803). The authors declare no conflict of interests.

REFERENCES

1. Hoffman, EP, Brown, RH Jr and Kunkel, LM (1987). Dystrophin: the protein product of the Duchenne muscular dystrophy locus. *Cell* **51**: 919–928.
2. Lu, QL, Rabinowitz, A, Chen, YC, Yokota, T, Yin, H, Alter, J *et al.* (2005). Systemic delivery of antisense oligoribonucleotide restores dystrophin expression in body-wide skeletal muscles. *Proc Natl Acad Sci USA* **102**: 198–203.
3. Malerba, A, Sharp, PS, Graham, IR, Arechavala-Gomeza, V, Foster, K, Muntoni, F *et al.* (2011). Chronic systemic therapy with low-dose morpholino oligomers ameliorates the pathology and normalizes locomotor behavior in mdx mice. *Mol Ther* **19**: 345–354.
4. Yokota, T, Lu, QL, Partridge, T, Kobayashi, M, Nakamura, A, Takeda, S *et al.* (2009). Efficacy of systemic morpholino exon-skipping in Duchenne dystrophy dogs. *Ann Neurol* **65**: 667–676.
5. Goemans, NM, Tulinius, M, van den Akker, JT, Burm, BE, Ekhart, PF, Heuvelmans, N *et al.* (2011). Systemic administration of PRO051 in Duchenne's muscular dystrophy. *N Engl J Med* **364**: 1513–1522.
6. Mendell, JR, Rodino-Klapac, LR, Sahenk, Z, Roush, K, Bird, L, Lowes, LP *et al.*; Eteplirsen Study Group. (2013). Eteplirsen for the treatment of Duchenne muscular dystrophy. *Ann Neurol* **74**: 637–647.
7. Voit, T, Topaloglu, H, Straub, V, Muntoni, F, Deconinck, N, Campion, G *et al.* (2014). Safety and efficacy of drisapersen for the treatment of Duchenne muscular dystrophy (DEMAND II): an exploratory, randomised, placebo-controlled phase 2 study. *Lancet Neurol* **13**: 987–996.
8. Malerba, A, Boldrin, L and Dickson, G (2011). Long-term systemic administration of unconjugated morpholino oligomers for therapeutic expression of dystrophin by exon skipping in skeletal muscle: implications for cardiac muscle integrity. *Nucleic Acid Ther* **21**: 293–298.
9. Wu, B, Lu, P, Benrashid, E, Malik, S, Ashar, J, Doran, TJ *et al.* (2010). Dose-dependent restoration of dystrophin expression in cardiac muscle of dystrophic mice by systemically delivered morpholino. *Gene Ther* **17**: 132–140.
10. Malerba, A, Kang, JK, McClorey, G, Saleh, AF, Popplewell, L, Gait, MJ *et al.* (2012). Dual Myostatin and Dystrophin Exon Skipping by Morpholino Nucleic Acid Oligomers Conjugated to a Cell-penetrating Peptide Is a Promising Therapeutic Strategy for the Treatment of Duchenne Muscular Dystrophy. *Mol Ther Nucleic Acids* **1**: e62.
11. Yin, H, Moulton, HM, Seow, Y, Boyd, C, Boutilier, J, Iverson, P *et al.* (2008). Cell-penetrating peptide-conjugated antisense oligonucleotides restore systemic muscle and cardiac dystrophin expression and function. *Hum Mol Genet* **17**: 3909–3918.
12. Wu, B, Cloer, C, Lu, P, Milazi, S, Shaban, M, Shah, SN *et al.* (2014). Exon skipping restores dystrophin expression, but fails to prevent disease progression in later stage dystrophic dko mice. *Gene Ther* **21**: 785–793.
13. McPherron, AC, Lawler, AM and Lee, SJ (1997). Regulation of skeletal muscle mass in mice by a new TGF-beta superfamily member. *Nature* **387**: 83–90.
14. Li, ZB, Kollias, HD and Wagner, KR (2008). Myostatin directly regulates skeletal muscle fibrosis. *J Biol Chem* **283**: 19371–19378.
15. Kang, JK, Malerba, A, Popplewell, L, Foster, K and Dickson, G (2011). Antisense-induced myostatin exon skipping leads to muscle hypertrophy in mice following octa-guanidine morpholino oligomer treatment. *Mol Ther* **19**: 159–164.
16. Kemaladewi, DU, Hoogaars, WM, van Heiningen, SH, Terlouw, S, de Gorter, DJ, den Dunnen, JT *et al.* (2011). Dual exon skipping in myostatin and dystrophin for Duchenne muscular dystrophy. *BMC Med Genomics* **4**: 36.
17. Merrick, D, Stadler, LK, Larner, D and Smith, J (2009). Muscular dystrophy begins early in embryonic development deriving from stem cell loss and disrupted skeletal muscle formation. *Dis Model Mech* **2**: 374–388.
18. Torres, LF and Duchen, LW (1987). The mutant mdx: inherited myopathy in the mouse. Morphological studies of nerves, muscles and end-plates. *Brain* **110 (Pt 2)**: 269–299.
19. Sharp, PS, Bye-a-Jee, H and Wells, DJ (2011). Physiological characterization of muscle strength with variable levels of dystrophin restoration in mdx mice following local antisense therapy. *Mol Ther* **19**: 165–171.
20. Dumonceaux, J, Marie, S, Beley, C, Trollet, C, Vignaud, A, Ferry, A *et al.* (2010). Combination of myostatin pathway interference and dystrophin rescue enhances tetanic and specific force in dystrophic mdx mice. *Mol Ther* **18**: 881–887.
21. Wagner, KR, Fleckenstein, JL, Amato, AA, Barohn, RJ, Bushby, K, Escolar, DM *et al.* (2008). A phase I/IItrial of MYO-029 in adult subjects with muscular dystrophy. *Ann Neurol* **63**: 561–571.
22. Krivickas, LS, Walsh, R and Amato, AA (2009). Single muscle fiber contractile properties in adults with muscular dystrophy treated with MYO-029. *Muscle Nerve* **39**: 3–9.
23. Arounleut, P, Bialek, P, Liang, LF, Upadhyay, S, Fulzele, S, Johnson, M *et al.* (2013). A myostatin inhibitor (propeptide-Fc) increases muscle mass and muscle fiber size in aged mice but does not increase bone density or bone strength. *Exp Gerontol* **48**: 898–904.
24. Pastoret, C and Sebille, A (1995). mdx mice show progressive weakness and muscle deterioration with age. *J Neurol Sci* **129**: 97–105.
25. Mosher, DS, Quignon, P, Bustamante, CD, Sutter, NB, Mellersh, CS, Parker, HG *et al.* (2007). A mutation in the myostatin gene increases muscle mass and enhances racing performance in heterozygote dogs. *PLoS Genet* **3**: e79.
26. Grobet, L, Martin, LJ, Poncelet, D, Pirottin, D, Brouwers, B, Riquet, J *et al.* (1997). A deletion in the bovine myostatin gene causes the double-muscled phenotype in cattle. *Nat Genet* **17**: 71–74.
27. McPherron, AC and Lee, SJ (1997). Double muscling in cattle due to mutations in the myostatin gene. *Proc Natl Acad Sci USA* **94**: 12457–12461.
28. Schuelke, M, Wagner, KR, Stolz, LE, Hübner, C, Riebel, T, Kömen, W *et al.* (2004). Myostatin mutation associated with gross muscle hypertrophy in a child. *N Engl J Med* **350**: 2682–2688.
29. Betts, C, Saleh, AF, Arzumanov, AA, Hammond, SM, Godfrey, C, Coursindel, T *et al.* (2012). Pip6-PMO, A New Generation of Peptide-oligonucleotide Conjugates With Improved Cardiac Exon Skipping Activity for DMD Treatment. *Mol Ther Nucleic Acids* **1**: e38.